Guo et al. BMC Cancer (2025) 25:605
https://doi.org/10.1186/s12885-025-14002-5

BMC Cancer

RESEARCH Open Access

Microwave ablation of non-small cell lung cancer enhances local T-cell abundance and alters monocyte interactions

Run-Qi Guo[1*], Yuan-Ming Li[1], Zhi-Xin Bie[1], Jin-Zhao Peng[1,2] and Xiao-Guang Li[1*]

Abstract

Background Minimally invasive thermal therapies show great prospect in non-small cell lung cancer (NSCLC) treatment. However, changes in immune cell populations following microwave ablation (MWA) in NSCLC microenvironment are not fully revealed.

Objective The present study was conducted to identify changes in immune cell populations and analyse dysregulated genes in immune cells after MWA in NSCLC microenvironment.

Methods The patients received fractionated MWA in two treatments separated by 3 weeks. Tumor biopsy samples were obtained through core-needle biopsy before each fractionated MWA procedure at the same site and used for single-cell RNA sequencing with the 10x Genomics pipeline.

Results A total of 9 major cell types were identified after MWA, which include neutrophils, T cells, B cells, monocytes, epithelial cells, chondrocytes, macrophages, tissue stem cells, and endothelial cells. After MWA, the tumor tissue exhibited an increased proportion of T cells. MWA altered gene expression in each cell cluster at the single-cell level. Cell trajectory analysis revealed that the cells at the starting point were most like T helper cells, naïve T cells, and regulatory T cells; they then developed into anergic T cells, T follicular cells, natural killer T cells, T memory cells, and exhausted T cells, and finally ended as γδ T cells and cytotoxic T cells. Moreover, after MWA, more interaction between monocytes and T cells (or B cells) were identified.

Conclusions MWA increases local T-cell abundance and alters monocyte interactions, thereby reshaping the tumor microenvironment. This study lays a foundation for investigating dysregulated genes that may contribute to the MWA-induced immune response in NSCLC.

What is already known on this topic Thermal ablation may change the immune profiles of patients by activating various steps in the cancer immunity cycle. However, changes in immune cell populations following MWA of NSCLC have not been fully reported.

*Correspondence:
Run-Qi Guo
lawlietkaku@gmail.com
Xiao-Guang Li
xglee88@126.com

Full list of author information is available at the end of the article

What this study adds After MWA, an increase in interactions between monocytes and T cells intratumorally was observed, which promoted antitumor immunity.

How this study might affect research, practice or policy The current study illuminates the MWA-caused systemic immune response in NSCLC, which may help to identify the dysregulated genes involved in the MWA-caused immune response.

Keywords Immune response, Lung cancer, Microwave ablation, T cells

Introduction

Lung malignancy is main cause of cancer-specific mortality worldwide, and non-small cell lung cancer (NSCLC) accounts for more than 80% of lung cancer cases [1]. Patients with early-stage NSCLC have better clinical outcomes. However, most patients are diagnosed with advanced NSCLC, and the median overall survival achieved approximately 12 months with concurrent chemoradiotherapy [2]. The development of immunotherapies has improved the survival in some patients. However, not all patients respond to immunotherapies, and even those who do respond can develop resistance [3, 4]. New approaches are needed to amply utilize the benefits of immunotherapy [5].

Thermal ablation consists of microwave ablation (MWA), cryoablation, and radiofrequency ablation (RFA), which are alternative options for curative-intent treatment in inoperable patients with early-stage NSCLC [6]. A few retrospective studies have shown comparable overall survival benefits for thermal ablation and stereotactic body radiation therapy [7, 8]. A 5-year overall survival rate of 27–67% have been reported for MWA, RFA, and cryoablation [9, 10], which are comparable to those of radiotherapy [11].

In addition, thermal ablation may change the immune profiles of patients by activating various steps in the cancer immunity cycle [12, 13]. In situ tumor ablation can generate a source of tumor-specific antigens [14] that are presented to lymphocytes by dendritic cells and macrophages [15]. Although evidence for this phenomenon is limited in NSCLC, immunogenic changes following thermal ablation have been reported in several malignancies. Generally, after RFA of solid tumors, a weak adaptive immune response can be found [16]. Due to its advantages over other ablative modalities in terms of accuracy and ablation zone size, MWA has been used to treat early-stage NSCLC [17].

Single-cell RNA sequencing (scRNA-seq) allows unprecedented comprehensive profiling of the immune system, providing potential targets for novel immunotherapy strategies [18]. In this study, scRNA-seq was conducted based on tumor tissue samples collected from 4 patients before and after MWA to explore the influence of MWA on immune cell populations in the tumor microenvironment of NSCLC. In this way, we illustrated transcriptome features of immune cells and stromal cells comprehensively, and we identified enhancement of local T-cell abundance and alternation of monocyte interactions after MWA, providing promising insight into the impact of MWA on immune cell populations and aberrantly expressed genes in the tumor microenvironment of NSCLC.

Materials and methods

Patients and tissue sampling

The study was authorized by Beijing Hospital's institutional ethics committee (2020BJYYEC-268-01), and all subjects provided signed informed permission. All procedures were performed following the Helsinki Declaration principles. Four patients received fractionated MWA in two treatments separated by 3 weeks. Tumor biopsy samples were obtained through core-needle biopsy from the same site before each fractionated MWA procedure and subjected to scRNA-seq.

The enrolled criteria for tumor samples are as following: (i) NSCLC diagnosed by core-needle biopsy; (ii) the greatest diameter is 3.0 cm or more confirmed by computed tomography, demonstrating the need for fractionated MWA; (iii) patients (older than 18 years) without chronic liver disease, coagulative disease, immune system diseases, renal failure or other diseases that could affect the immune response.

Preparation for single-cell suspensions

Tumor biopsy tissues were transported immediately after biopsy in ice-cold H1640 (Gibco, Life Technologies, NY, USA) and cleaned with phosphate-buffered saline (PBS; Thermo Fisher Scientific, NY, USA). Then, the tumor biopsy tissues were grinded using the ULTRA-TURRAX® Tube Drive disperser (IKA, Germany). Next, filtering of the digested tissues was performed using a nylon mesh (70 μm). Following centrifugation, the pelleted cells were suspended in ice-cold red blood cell lysis buffer (Solarbio, Beijing, China) followed by filtering with a nylon mesh (40 μm). Finally, the pelleted cells were resuspended in Dulbecco's PBS (1 ml; Solarbio, Beijing, China), and then an automatic cell counter (Countstar, USA) was applied to measure the concentration of clumped cells and live cells.

Droplet-based single-cell RNA-sequencing (Drop-seq)

After cell suspension was loaded on Chromium single-cell controller (10X Genomics), the Chromium™ Single Cell A Chip Kit (10X Genomics, Pleasanton, CA) and Single Cell 3'Library & Gel Bead Kit V2 (10X Genomics) were used following the product instruction to make single-cell gel beads in emulsion (GEMs). Single cells were suspended in PBS with bovine serum albumin (0.04%). Each channel received roughly 1×10^4 cells, with $\sim 6 \times 10^3$ cells retrieved. After the lysis of collected cell samples, the liberated RNA was coded in individual GEMs using reverse transcription at 53 °C for 45 min, followed by 5 min at 85 °C, with a final holding at 4°C. The quality of synthesized complementary DNA was determined by the Agilent 4200 system (done by CapitalBio Technology, Beijing, China) in accordance with the instructions. The Single Cell 3'Library Gel Bead Kit V2 (10X Genomics) was applied to create scRNA-seq libraries. The libraries were sequenced using the NovaSeq 6000 system (Illumine, San Diego, CA, USA) with a 150-base pair (PE150) reading method.

Data processing for scRNA-seq

Cell Ranger (version 2.2.0) Pipeline was used in conjunction with GRCh38 (human reference genome assembly) to produce raw gene expression matrix for each sample. After empty droplets were removed using the DropletUtils [19] package (version 1.2.2), R software (version 3.5.3) with the Seurat package (version 3.0.0) [20] were used to analyse the output-filtered gene expression matrix. In summary, genes accounting for at least 0.1% of all data and the cells expressing more than 200 genes were kept for following exploration. When cells had less than 500 unique molecular identifiers (UMIs), more than 6000 or less than 200 genes, or more than 10% UMIs generated from the mitochondrial genome, these cells were deleted. After removing the cells with low quality, the NormalizeData function was used to normalize the gene expression matrix, and with the FindVariableFeatures function, 2000 characteristics with high cell-to-cell variation were identified. The RunPCA function was used to reduce dataset dimensionality with default settings on linear transformation scaled data provided by the ScaleData function. Following that, the JackStrawPlot, DimHeatmap, and ElbowPlot were employed as indicated by the Seurat developers for identification of the true dataset dimensionality. Finally, the FindNeighbors and FindClusters were applied for cell clustering, and the RunUMAP with default values to do nonlinear dimensional reduction. All the details about the Seurat analyses used in the present study are available on the website (https://satijalab.org/seurat/v3.0/pbmc3k_tutorial.html).

Integration of datasets

The published method of integration (https://satijalab.org/seurat/v3.0/integration.html) [21] were used to compare cell kinds and proportions across the three circumstances. Many unique scRNA-seq datasets were integrated and unbatched using the Seurat package. In summary, as previously mentioned, 2000 characteristics with substantial cell-to-cell variation were identified. Finally, with the FindIntegrationAnchors function, "anchors" connecting various datasets were found and sent to the IntegrateData function for generation of a "batch-corrected" expression matrix for all cells, making cells from different datasets integrated and analysed together.

Interpretation of cell types and identification of cluster markers

UMAP was utilized for reduction of nonlinear dimensionality and projection of all cells to two-dimensional space. Then, based on their common features, the cells were clustered together. The FindAllMarkers function in Seurat was applied for localization of canonical cell-type markers in the detected clusters. Afterwards, according to the expression of these markers, the clusters can be categorized and interpreted. Clusters expressing two or more cell-type markers were labelled as doublet cells and those expressing no markers were labelled as cells with low quality, which were both removed from further investigation.

Subclustering of major cell types

After cells were initially extracted from the integrated dataset for each major type, subclustering of major cell types were then performed. Genes were scaled to unit variance after integration. The scaling, principal component analysis, and clustering were carried out as previously stated.

Identification of potential interactions among cell types

As described previously [22], potential interactions among various cell types were identified according to the expression of a receptor by one cell type and the expression of an interacting ligand by another cell type. Ramilowski et al. [23] provided the list of potential receptor-ligand interactions. A receptor or ligand transcript was regarded as "expressed" by a specific cell type when its average expression in the cell type was more than 0.5 on a $\log_2$ scale and its expression accounts for at least 10% of the cell type. When a cell type expressed the receptor or ligand, the related communication was labelled as incoming or outgoing for the cell type.

Gene set variation analysis

Pathway analysis was performed using the 50 hallmark pathways defined in the molecular signature database [24]. A dataset of 85 metabolic pathways was utilized for evaluation of metabolic pathway activity [25]. GSVA with standard settings was utilized to assign pathway activity as described previously [26] in the GSVA [27] R package (version 1.30.0). Calculation of the differential activities of pathways between clusters or circumstances was performed utilizing the Limma [28] R package (version 3.38.3). A Benjamini-Hochberg-corrected P value less than 0.01 was the threshold for significantly disrupted pathways.

Cell–cell interaction analysis

The cell–cell communications were identified using CellPhoneDB based on normalized UMI to determine the network among various cell clusters. Significant cell–cell interactions (P value of < 0.05) were investigated further. The network graphs of the cell–cell interactions were visualized and analysed using Cytoscape (San Francisco, CA, USA). A CellChat (version 0.0.2) was used for the analysis of intercellular communication networks derived from scRNA-seq. Using the R package procedure, a CellChat object was built. The object's meta variable now includes cell information. The database of ligand–receptor communication was created, and the matching receptor inference was calculated.

Diffusion map and pseudotime analysis

Diffusion mapping and pseudotime analysis were performed on single cells allocated to T-cell clusters. First, each cluster's differentially expressed genes were identified. Afterwards, these data were imported into the DiffusionMap function in the destiny R package (version 2.12.0). The diffusion map and pseudotime analyses were run using default settings. The root cell for diffusion pseudotime computation utilizing the first two diffusion components was a naïve T-cell [29–32].

Results

Study design and clinical characteristics of enrolled patients

To explore the local effect of MWA on immune cell populations in the tumor microenvironment of locally advanced NSCLC, tumor tissues were collected from 4 patients with NSCLC before the 1st and the 2nd MWA and then subject to the scRNA-seq (Fig. 1A). Among the 4 tumor samples (Fig. 1B), one sample exhibited EGFR exon 19 deletion, two samples were PD-L1 positive/TMB-high, and the rest one sample was driver-gene negative/PD-L1 negative/TMB-low. In one case, complete necrosis of the tumor occurred after the first MWA, and the core needle biopsy tissue collected after this treatment was therefore excluded for further scRNA-seq (Fig. 1B). Transcriptomic profiles from 51,250 cells were obtained after data processing.

The immune cell composition of tumor samples was altered after MWA

T-distributed stochastic neighbour embedding analysis was utilized to characterize the cell types presented in tumor tissue before and after MWA. After the identification of 23 high-confidence cell clusters (Fig. 2A, **left panel**) and their origins (Fig. 2A, **right panel**), all these clusters can be allocated to known cell lineages (Fig. 2B). A total of 9 major cell types were identified for the following study, which include neutrophils, T cells, B cells, monocytes, epithelial cells, chondrocytes, macrophages, tissue stem cells, and endothelial cells (Fig. 2C). After MWA, the tumor tissue exhibited an increased proportion of T cells and neutrophils and a reduced proportion

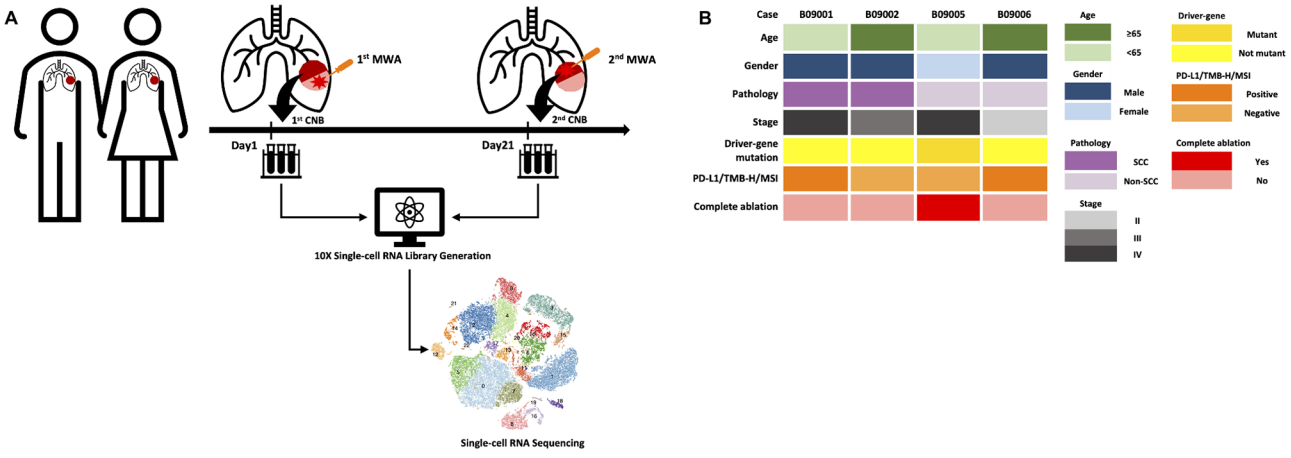

Fig. 1 Study design. **(A)** The timeline of human tissue collection, MWA, and the scRNA-seq. **(B)** Clinical characteristics of patients from whom tissue samples were collected

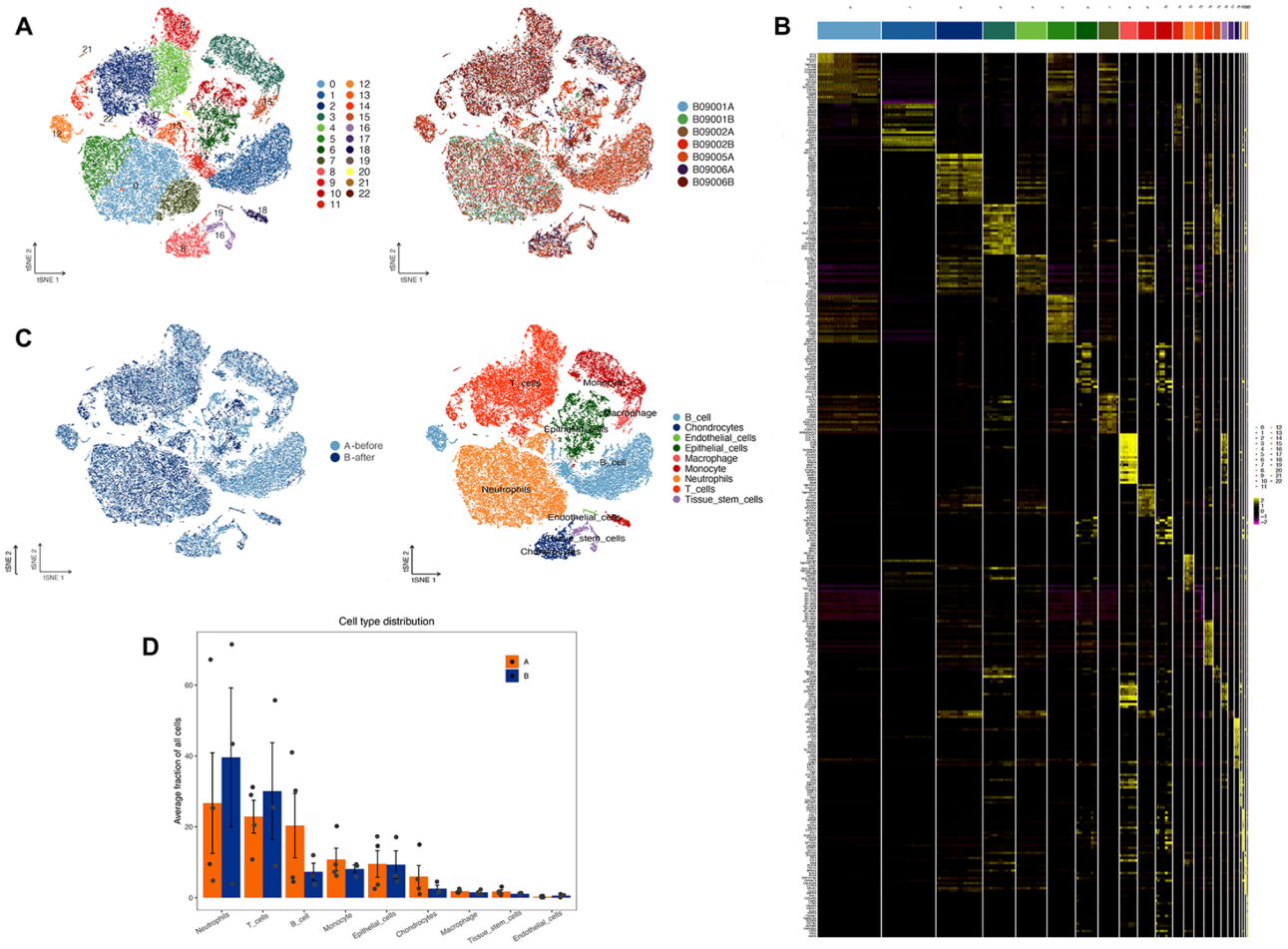

Fig. 2 ScRNA-seq of the MWA-caused intratumoral immune response in localized NSCLC. **(A)** T-distributed stochastic neighbour embedding plot shows cell types (the left panel) and cell origins by patient (the right panel). **(B)** A heatmap of the top 20 gene sets of each cluster from these 23 clusters. **(C)** The T-distributed stochastic neighbour embedding plot showing dynamic changes in MWA-stimulated intratumoral cells of NSCLC. **(D)** Histogram indicating the cell type distribution in 4 tumor samples before and after MWA

of B cells, monocytes, and chondrocytes, with stable proportions of epithelial cells, macrophages, tissue stem cells and endothelial cells (Fig. 2D).

Changes in intratumoral T cells after MWA in NSCLC tumor microenvironment

After MWA, expression levels of IGHG1, LGLC2, IGKC, IGHG3, IGLC3, IGLC1, IGHA1, IGHG4, HBB, and IGHG2 were reduced in T cells (Fig. 3A). The criteria for identifying these genes and their gene expression characteristics in T cells before and after MWA are shown in Supplementary Tables 1–2. Gene ontology enrichment analyses implied that the genes altered in intratumoral T cells after MWA were enriched in the cellular oxidant detoxification pathway, hydrogen peroxide catabolic process pathway, oxygen transport pathway, and tumor necrosis factor-activated receptor activity pathway (Fig. 3B). More precisely, the cellular oxidant detoxification pathway can maintain immune cell function and affect the differentiation and development of immune cells. Excessive accumulation of these oxidative substances can damage the structure and function of immune cells [33]. Antioxidant enzymes in the cellular oxidant detoxification pathway, such as superoxide dismutase (SOD), catalase (CAT), and glutathione peroxidase (GPx), can promptly remove ROS, ensuring that immune cells such as macrophages, T cells, and B cells can normally perform functions like phagocytosis, cytokine secretion, and antibody production [34]. In addition, a recent study reported that deactivating whole-cell bacteria using hydrogen peroxide is beneficial for the immune response [35]. Moreover, the phase transition of the PPO2 protein in Drosophila immune cells enables oxygen transport, which in turn helps maintain internal oxygen homeostasis, indicating the essential role of oxygen transport pathway in immune profile [36]. Furthermore, members of the tumor necrosis factor receptor superfamily play a key role in regulating both innate

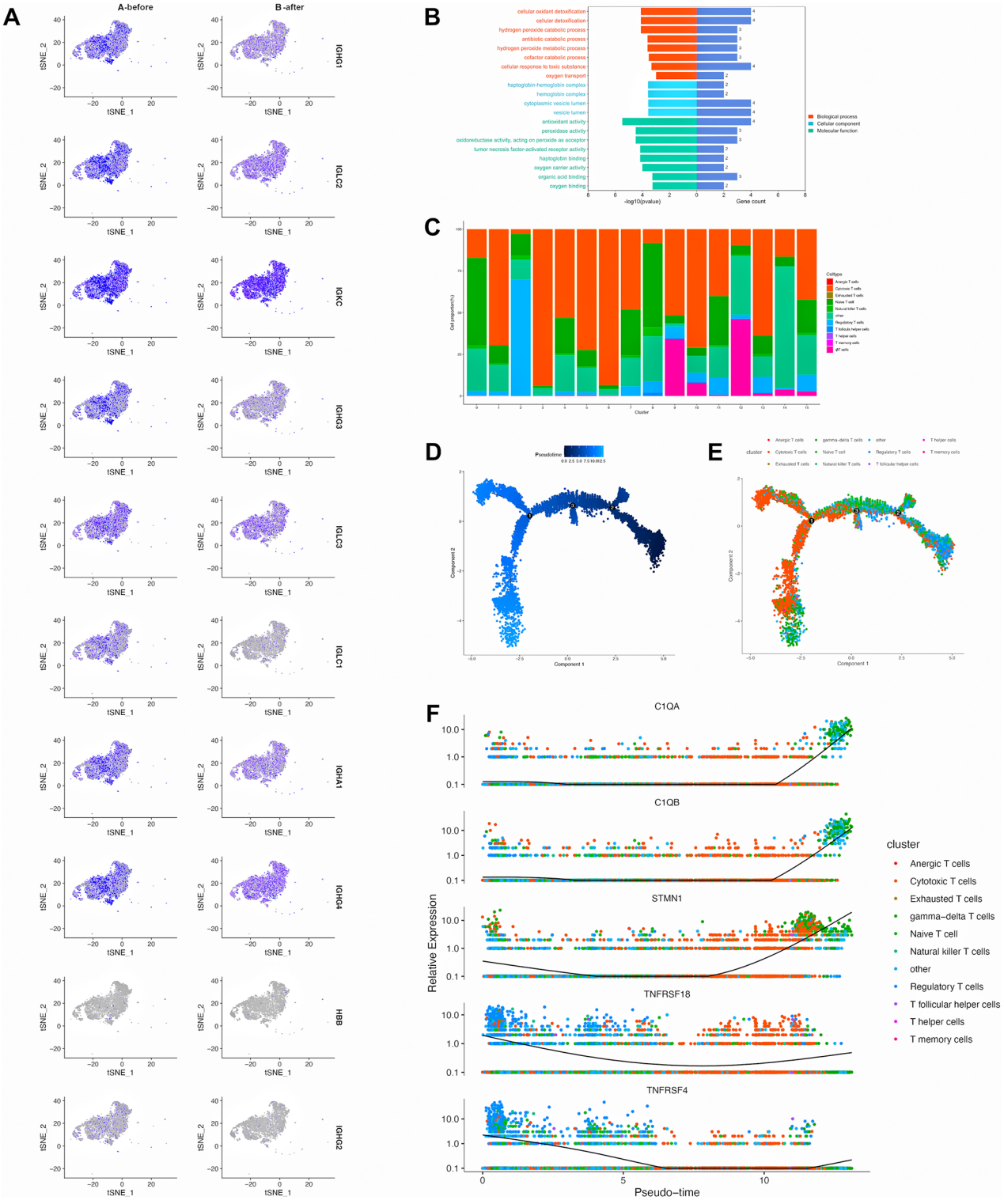

Fig. 3 Changes in intratumoral T cells and analysis of dysregulated genes in T cells after MWA. **(A)** Aberrantly expressed genes in T cells after MWA. **(B)** Gene Ontology enrichment analyses showing pathways that the dysregulated genes enriched in. **(C)** The proportion of each T-cell subtype in the clusters. **(D)** T-cell developmental trajectory plot with corresponding data analysis by Monocle 2. **(E)** T-cell subclusters established by Seurat overlaid on the Monocle 2 pseudotime plot. **(F)** Five genes that shows the most dynamic expression changes along the T-cell developmental trajectory

and adaptive immune cells. This regulation is essential for coordinating various mechanisms that either co-stimulate or co-inhibit the immune response [37]. Overall, these signaling pathways are closely related to immune profile by regulating immune cell function and participating in the immune response.

To characterize the MWA-induced T-cell response, these cells were reclustered and 11 major T-cell types were identified (Fig. 3C, Supplementary Table 3), including $BTLA^+ITCH^+NEDD4^+$ T cells (anergic T cells), $GZMB^+CD8A^+$ T cells (cytotoxic T cells), $LAG3^+$ T cells (exhausted T cells), $CCR7^+LEF1^+SELL^+TCF7^+$ T cells (naïve T cells), $SLAMF1^+SLAMF6^+$ T cells (natural killer T cells), $IL2RA^+IKZF2^+FOXP3^+$ T cells (regulatory T cells), $CD200^+ICOS^+P2RX7^+$ T cells (T follicular helper cells), $NR3C1^+CCR5^+CD3G^+$ T cells (T helper cells), $CD200^+ENPP1^+PTPRC^+$ T cells (T memory cells), $CCL5^+H2AFZ^+HMGB2^+S100B^+STMN1^+$ T cells (γδ T cells), and other rare cell types.

Furthermore, the Monocle 2 algorithm [38] was applied to order the T cells in pseudotime to define their developmental trajectories. Based on the expression signatures, the cells at the starting point of the trajectory were most like naïve T cells, regulatory T cells, and T helper cells; these cells then developed to anergic T cells, T follicular cells, natural killer T cells, T memory cells, and exhausted T cells, and the trajectory ended with γδ T cells and cytotoxic T cells (Fig. 3D-E). These findings suggest that MWA might enhance the antitumor immune response by regulating functional cytotoxic T-cell and γδ T-cell accumulation.

Subsequently, expression patterns of all genes along the T-cell developmental trajectory were analysed and five genes that showed the most dynamic expression changes were identified (Fig. 3F). Among the five genes, C1QA, C1QB and STMN1 were upregulated while TNFRSF18 and TNFRSF4 were downregulated in T cells. The significant upregulation or downregulation of these genes indicates the significant potential of these genes in regulating T cell behavior in the NSCLC tumor microenvironment after MWA.

Changes in intratumoral B cells after MWA

After MWA, B cells displayed the decreased expression of IGLC7, IGHG2, IGHG1, PERP, IGHG3, GZMB, ATF5, SPRR3, AKR1B10, and PTP4A3 (Fig. 4A). The criteria for recognizing these genes and their expression profile in B cells before and after MWA are shown in Supplementary Tables 4–5. Gene ontology enrichment analysis indicated that genes altered in intratumoral B cells after MWA were not only enriched in the cellular oxidant detoxification pathway and hydrogen peroxide catabolic process pathway, as those in T cells, but also enriched in the cellular response to interleukin 4 (Fig. 4B) which is closely involved in immune response and is highly expressed in the tumor microenvironments of different types of cancer. Gene expression data of B cells were projected utilizing diffusion maps, and six B-cell clusters were identified through scRNA-seq (Supplementary Table 6), including $CXCR4^+$ B cells (trafficking B cells), $IL7R^+PAX5^+$ B cells (pro B cells), $CD24^+CD27^+CD38^+CD40^+IL4R^+IL7R^+$ B cells (immature B cells), $BIRC3^+CD52^+HLA\text{-}DQB1^+SELL^+$ B cells (naïve B cells), $LMO2^+$ B cells (germinal centre B cells), and $IGHG1^+MZB1^+SSR4^+$ B cells (plasma cells) (Fig. 4C). Moreover, annotation results for single-cell types (T cells or B cells) are shown in Supplementary Table 7.

Characterization of cell–cell interactions

CellPhoneDB was used to analyse cell–cell communications that might improve the MWA-caused immune responses. Before and after MWA, the communications among cell types were completely analysed. Monocytes are direct progenitors of macrophages derived from haematopoietic stem cells, and the presence of macrophages correlates with a decreased survival in the majority of cancers [39]. After MWA, there was less interaction between monocytes and macrophages than that before MWA (Fig. 5A). Intratumorally, more communications between monocytes and T cells (or B cells) after MWA were identified (Fig. 5A). According to previous studies, signals from the tumor microenvironment can transfer monocytes and their derivatives into macrophages that assist tumor cells in evading cytotoxic T cells [40, 41]. In addition, a higher prescence of $CD8^+$ T cells within tumors is linked to more favorable outcomes in cancer patients [42]. Therefore, understanding the interactions between monocytes and T cells within these niches could therefore guide the development of therapeutic strategies for cancer and other immunological diseases. Monocytes are crucial in modulating the inflammatory microenvironment both within and surrounding tumors [43]. These cells can be recruited to the tumor site, where they contribute to the inflammatory milieu, which in turn significantly influences B cell function [44]. CX3CL1 is a chemokine that exhibits potent chemotactic activity for many immune cells including human monocytes, T cells and B cells. Its diverse roles render it an attractive candidate for therapeutic development [44]. Consequently, identifying additional molecules such as CX3CL1 that modulate the interactions among various immune cells is critical for advancing therapeutic strategies in NSCLC. In this study, increased communications between monocytes and T cells (or B cells) via CD55-ADGRE5, TNFRSF1B-GRN, and LGALS9-CD44 were observed after MWA compared to the interactions before MWA (Fig. 5B). In addition, a strong interaction between monocytes and T cells (or B cells) via

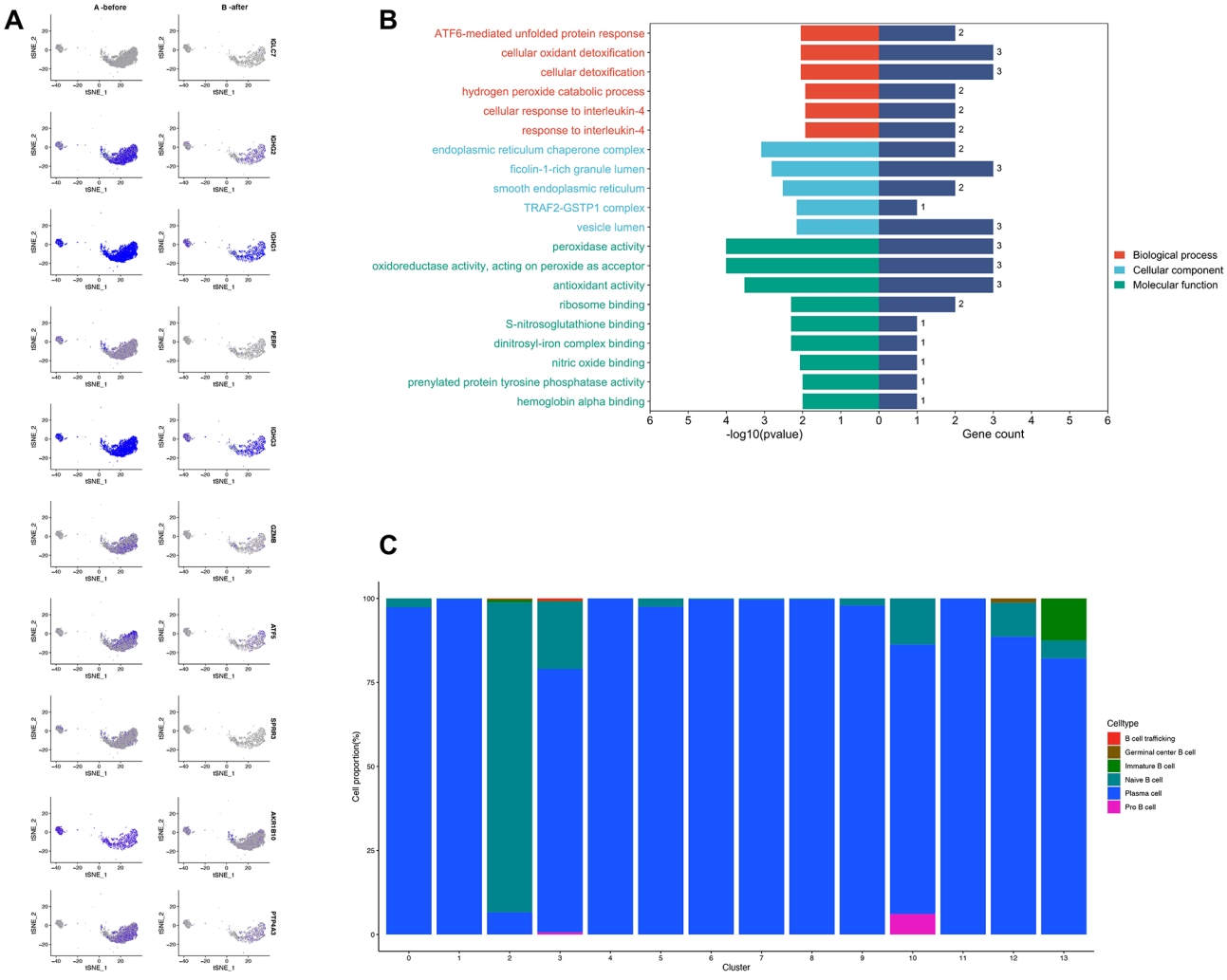

Fig. 4 Analysis of aberrantly expressed genes in intratumoral B cells and changes in B cell subtypes after MWA. **(A)** Identification of abnormally expressed genes in B cells after MWA. **(B)** Gene Ontology enrichment analysis showing pathways that these dysregulated genes after MWA enriched in. **(C)** The proportion of each B-cell subtype in the clusters

C5AR1-RPS19 was persisted and remained unaffected by MWA (Fig. 5B). Previously, the levels of CD55 and CD59 are negatively correlated with the infiltration of M1 macrophages and CD8 + T cells in human lung cancer specimens, and these levels serve as predictors of patient outcomes [45]. C5AR1 is an immune-regulatory protein, and $CD3^{+}C5AR1^{+}$ is higher in early-stage NSCLC than healthy volunteers [46]. The role of TNFRSF1B and LGALS9 in NSCLC is limitedly reported and requires more investigation in the future.

Discussion

Immunotherapy has become a powerful and promising clinical strategy for NSCLC treatment [47]. It is of the utmost importance to develop adjuvant therapies so that the benefits of immunotherapy can be enlarged. Thermal ablative methods could enhance anticancer immune response, and the combination of thermal ablative modality and immunotherapy has the potential to be an effective strategy [48]. The features of the MWA-caused immune response in breast cancer were reported by Zhou et al. [49]. However, the immune response induced by MWA in NSCLC has not been completely characterized.

In most cases, localized NSCLC can be cured by resecting the primary tumor and then using systemic treatment. Nevertheless, relapses are often recognized in patients with NSCLC, which might be attributed to circulating tumor cells as well as the development of an immunosuppressive microenvironment. Incomplete thermal ablation has been shown to induce immunosuppression in preclinical studies, and a decreased proportion of natural killer cells and T cells was observed in one tumor with incomplete thermal ablation [50]. In the present study, it was found that T-cell proportion, especially the number of functional cytotoxic T cells and γδ T cells,

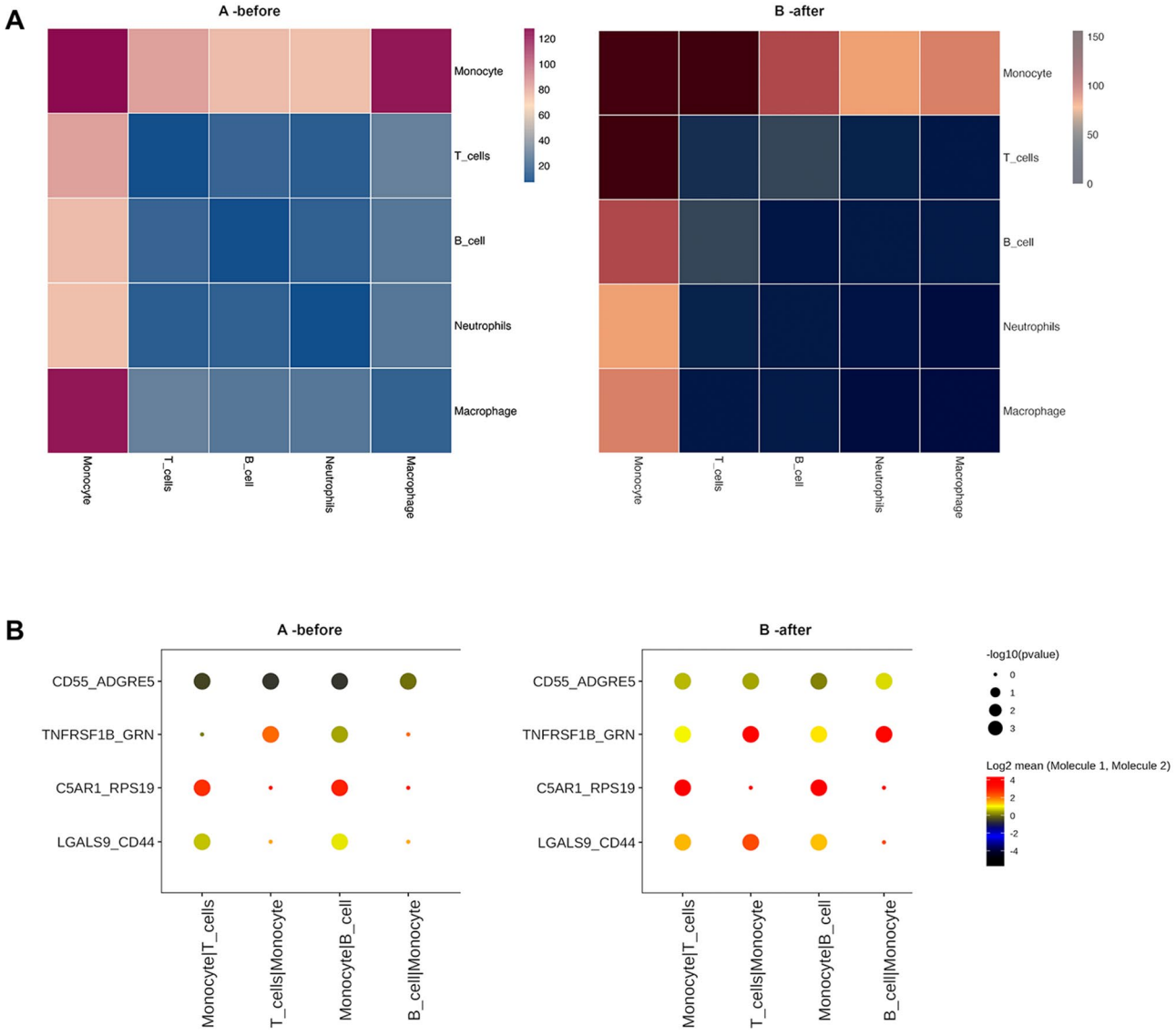

Fig. 5 Cell–cell communications among intratumoral immune cells before and after MWA for the treatment of NSCLC. **(A)** Before and after MWA, the cell–cell interactions among the intratumoral immune cells. **(B)** Illustration of the ligand–receptor interactions between monocytes and T cells (or B cells) before MWA (the left panel) and after MWA (the right panel)

was increased after MWA of NSCLC. Cytotoxic T cells act as essential cellular mediators of immune defense against malignant cells and intracellular pathogens [51]. γδ T cells are enriched in many peripheral tissues, including lung, intestine, and skin, and these cells contribute to immune response by rapidly producing numerous cytokines [52]. γδ T cells can directly recognize tumor cells through T cell receptor and natural killer cell receptors [53]. Therefore, it can be concluded that MWA treatment enhances the antitumor immune response by augmenting the accumulation of functional cytotoxic T-cells and γδ T-cells. Despite T cells, neutrophils are also accumulated in lung samples after MWA. Neutrophils have the ability to infiltrate into tumors and participate in tumor progression. They can be regarded as potential targets in cancer treatment because they can diminish oncogenic pathways by regulating immune checkpoint blockade [54]. Moreover, our study revealed that the proportion of B cells, monocytes, and chondrocytes was significantly reduced after MWA of NSCLC. B cells play a dual role in lung cancer [55], and different monocyte subsets facilitate pro-tumor or anti-tumor immunity [56], which are associated with complex mechanisms.

Many genes were discovered to be aberrantly decreased in T cells and B cells after MWA. IGHG1, IGHG2, and IGHG3 were downregulated in both T cells and B cells after MWA treatment. According to previous studies, IGHG1 is highly expressed in glioma, and its expression

is positively correlated to immune score and negatively associated with tumor purity [57]. IGHG2 displays low expression in sarcoma cells compared to that in skeletal muscle cells [58]. IGHG3 is highly expressed in serum samples from NSCLC patients responding to chemotherapy compared with non-responders [59]. Other genes such as IGKC is a strong prognostic marker in solid tumors including lung cancer [60]. IGHA1, IGLC3, and IGKC are regarded as marker genes in immune cells of lung adenocarcinoma [61].

Furthermore, after MWA, a stronger communication between monocytes and T cells (or B cells) was intratumorally observed, for example, CD55-ADGRE5, TNFRSF1B-GRN, and LGALS9-CD44, and the phenomenon promoted antitumor immunity. CD55 is known as a decay-accelerating factor, which is a complement regulatory protein expressed on most cells to defend them against complement-induced attack. It was discovered that the interaction of CD55-ADGRE5 (CD97) between monocytes and T cells (or B cells) was enhanced, and the finding is consistent with that of a published article. Melania Capasso et al. reported that because the binding of CD55 to ADGRE5, an EGF-TM7 receptor constitutively shows expression on granulocytes and monocytes and is promptly upregulated on T and B cells upon activation [62]. MWA also increased the TNFRSF1B (TNF receptor 2)-GRN (growth factor progranulin). The overexpression of TNFRSF1B in some tumor cells and its critical role in immunosuppressive cells, particularly in regulatory T cells, makes blocking TNFR2 an excellent cancer treatment strategy [63]. GRN has previously been shown to be a ligand of TNFR, which is an antagonist of TNFα signalling [64]. As a result, the improved interaction may also promote an antitumor immune response. LGALS9 (galectin 9) also promotes T-cell activation via CD44 binding and LCK signalling [65]. Monocytes and T cells showed increased LGALS9-CD44 interaction. Moreover, CD44 clustering and cross-linking can influence T-cell signalling by stabilizing LCK activation and protein kinase C-mediated movement according to a previous study [66].

On the other hand, a RPS19-C5AR1 (strong ribosome protein S19 - complement C5a receptor 1) communication between monocytes and T cells (or B cells) was identified both before and after MWA, which can upregulate immunosuppressive signalling [67]. RPS19 is upregulated in cancer cells and can be released from apoptotic tumor cells, thereby interacting with complement C5AR1 which is expressed on tumor-infiltrating myeloid-derived suppressor cells. The communication contributes to tumor growth by making it easier for these cells to be recruited to the tumor. RPS19 can also stimulate the release of immunosuppressive agents, such as TGF-β, by myeloid-derived suppressor cells in tumor-draining lymph nodes, resulting in Th2-biased T-cell responses. In addition, RPS19 facilitates the production of regulatory T cells and inhibits $CD8^+$ T-cell infiltration into tumors [68]. Interrupting the RPS19-C5AR1 interaction has been shown to increase $CD8^+$ T-cell infiltration in cancers [68].

The limitations of the present study are listed as follow. First, immune response was determined in a short term; future research should focus on the long-term immune response. Second, the MWA-induced immune response begins with local antigen processing and presentation. However, due to the difficulty of obtaining drainage lymph node samples, the features of the initial immune process were not explored. Third, due to the small sample size, our findings do not consider various clinicopathological factors and various local controls. Moving forward, for the purpose of determining the potential patients who could benefit from this local therapy with an additional enhanced immune response, studies with larger sample sizes are required. Fourth, it is still unclear whether MWA's antitumor activity is enhanced when combined with immune checkpoint inhibitors. Additional clinical trials will need to be conducted in the future.

Conclusions

The current study illuminates the characteristics of the MWA-caused immune response in NSCLC. MWA enhances local T-cell abundance and alters monocyte interactions. This study provides a basis for identifying and exploring the functions and mechanisms of possible targets to improve MWA-caused immune response in NSCLC.

Supplementary Information

The online version contains supplementary material available at https://doi.org/10.1186/s12885-025-14002-5.

Supplementary Table 1. Differences in top genes in T cells before and after ablation

Supplementary Table 2. Top gene expression characteristics in T cells before and after ablation

Supplementary Table 3. Classification of T cell subsets using cell marker genes

Supplementary Table 4. Differences in top genes of B cells before and after ablation

Supplementary Table 5. Top gene expression features of B cells before and after ablation

Supplementary Table 6. Classification of B cell subsets using cell marker genes

Supplementary Table 7. Annotation results for single-cell types (B cells or T cells)

Author contributions

R.Q.G. and X.G.L. designed the research and supervised the study. Y.M.L., Z.X.B., and J.Z.P. performed the experiments. R.Q.G. was responsible for the

bioinformatics analysis and the writing of the manuscript. X.G.L. revised the manuscript. The final manuscript was read and approved by all authors.

Funding
This study is supported by Beijing Hospital Pre-research Project for National Natural Science Foundation of China under Grant BJ-2020-133 and Fundamental Research Funds for Central University (No. 3332023091) under Grant BJ-2023-275.

Data availability
Link: https://pan.baidu.com/s/1bjN4mklyFXgOd3ETjLnA1g?pwd=8944 Code: 8944.

Declarations

Ethical approval
The Ethics Review Board of Beijing Hospital approved the study (Approval Number: 2020BJYYEC-268-01).

Consent to participate
All procedures associated with human participants were conducted following the Helsinki declaration principles. Written informed consent was obtained from all patients from whom tumor tissues were collected.

Competing interests
The authors declare no competing interests.

Author details
[1]Minimally Invasive Tumor Therapies Centre Beijing Hospital, Institute of Geriatric Medicine, National Centre of Gerontology, Chinese Academy of Medical Sciences, No.1 Dongdan Dahua Street, Beijing 100370, P.R. China
[2]Graduate School of Peking Union Medical College, Chinese Academy of Medical Sciences, Beijing, P.R. China

Received: 23 April 2024 / Accepted: 24 March 2025
Published online: 03 April 2025

References

1. Suster DI, Mino-Kenudson M. Molecular pathology of primary Non-small cell lung cancer. Arch Med Res. 2020;51(8):784–98.
2. Reck M, Rabe KF. Precision diagnosis and treatment for advanced Non-Small-Cell lung cancer. N Engl J Med. 2017;377(9):849–61.
3. Lievense LA, Sterman DH, Cornelissen R, Aerts JG. Checkpoint Blockade in lung cancer and mesothelioma. Am J Respir Crit Care Med. 2017;196(3):274–82.
4. Gettinger SN, Wurtz A, Goldberg SB, et al. Clinical features and management of acquired resistance to PD-1 axis inhibitors in 26 patients with advanced Non-Small cell lung cancer. J Thorac Oncol. 2018;13(6):831–9.
5. Rangamuwa K, Leong T, Weeden C, et al. Thermal ablation in non-small cell lung cancer: a review of treatment modalities and the evidence for combination with immune checkpoint inhibitors. Transl Lung Cancer Res. 2021;10(6):2842–57.
6. Postmus PE, Kerr KM, Oudkerk M, et al. Early and locally advanced non-small-cell lung cancer (NSCLC): ESMO clinical practice guidelines for diagnosis, treatment and follow-up. Ann Oncol. 2017;28(suppl4):iv1–21.
7. Uhlig J, Ludwig JM, Goldberg SB, Chiang A, Blasberg JD, Kim HS. Survival rates after thermal ablation versus stereotactic radiation therapy for stage 1 Non-Small cell lung cancer: A National cancer database study. Radiology. 2018;289(3):862–70.
8. Yuan Z, Wang Y, Zhang J, Zheng J, Li W. A Meta-Analysis of clinical outcomes after radiofrequency ablation and microwave ablation for lung cancer and pulmonary metastases. J Am Coll Radiol. 2019;16(3):302–14.
9. Lam A, Yoshida EJ, Bui K, et al. Patient and facility demographics related outcomes in Early-Stage Non-Small cell lung cancer treated with radiofrequency ablation: A National cancer database analysis. J Vasc Interv Radiol. 2018;29(11):1535–e15411532.
10. Ni Y, Huang G, Yang X, et al. Microwave ablation treatment for medically inoperable stage I non-small cell lung cancers: long-term results. Eur Radiol. 2022;32(8):5616–22.
11. Chi A, Fang W, Sun Y, Wen S. Comparison of Long-term survival of patients with Early-Stage Non-Small cell lung cancer after surgery vs stereotactic body radiotherapy. JAMA Netw Open. 2019;2(11):e1915724.
12. Takaki H, Cornelis F, Kako Y, Kobayashi K, Kamikonya N, Yamakado K. Thermal ablation and Immunomodulation: from preclinical experiments to clinical trials. Diagn Interv Imaging. 2017;98(9):651–9.
13. Katzman D, Wu S, Sterman DH. Immunological aspects of cryoablation of Non-Small cell lung cancer: A comprehensive review. J Thorac Oncol. 2018;13(5):624–35.
14. den Brok MH, Sutmuller RP, van der Voort R, et al. In situ tumor ablation creates an antigen source for the generation of antitumor immunity. Cancer Res. 2004;64(11):4024–9.
15. Yu M, Pan H, Che N, et al. Microwave ablation of primary breast cancer inhibits metastatic progression in model mice via activation of natural killer cells. Cell Mol Immunol. 2021;18(9):2153–64.
16. Mizukoshi E, Yamashita T, Arai K, et al. Enhancement of tumor-associated antigen-specific T cell responses by radiofrequency ablation of hepatocellular carcinoma. Hepatology. 2013;57(4):1448–57.
17. Lubner MG, Brace CL, Hinshaw JL, Lee FT Jr. Microwave tumor ablation: mechanism of action, clinical results, and devices. J Vasc Interv Radiol. 2010;21(8 Suppl):S192–203.
18. Papalexi E, Satija R. Single-cell RNA sequencing to explore immune cell heterogeneity. Nat Rev Immunol. 2018;18(1):35–45.
19. Lun ATL, Riesenfeld S, Andrews T, et al. EmptyDrops: distinguishing cells from empty droplets in droplet-based single-cell RNA sequencing data. Genome Biol. 2019;20(1):63.
20. Butler A, Hoffman P, Smibert P, Papalexi E, Satija R. Integrating single-cell transcriptomic data across different conditions, technologies, and species. Nat Biotechnol. 2018;36(5):411–20.
21. Stuart T, Butler A, Hoffman P, et al. Comprehensive integration of Single-Cell data. Cell. 2019;177(7):1888–902. e1821.
22. Puram SV, Tirosh I, Parikh AS, et al. Single-Cell transcriptomic analysis of primary and metastatic tumor ecosystems in head and neck cancer. Cell. 2017;171(7):1611–e16241624.
23. Ramilowski JA, Goldberg T, Harshbarger J, et al. A draft network of ligand-receptor-mediated multicellular signalling in human. Nat Commun. 2015;6:7866.
24. Subramanian A, Tamayo P, Mootha VK, et al. Gene set enrichment analysis: a knowledge-based approach for interpreting genome-wide expression profiles. Proc Natl Acad Sci U S A. 2005;102(43):15545–50.
25. Xiao Z, Dai Z, Locasale JW. Metabolic landscape of the tumor microenvironment at single cell resolution. Nat Commun. 2019;10(1):3763.
26. Lambrechts D, Wauters E, Boeckx B, et al. Phenotype molding of stromal cells in the lung tumor microenvironment. Nat Med. 2018;24(8):1277–89.
27. Hänzelmann S, Castelo R, Guinney J. GSVA: gene set variation analysis for microarray and RNA-seq data. BMC Bioinformatics. 2013;14:7.
28. Ritchie ME, Phipson B, Wu D, et al. Limma powers differential expression analyses for RNA-sequencing and microarray studies. Nucleic Acids Res. 2015;43(7):e47.
29. Wu J, Zhao X, Sun Q, et al. Synergic effect of PD-1 Blockade and endostar on the PI3K/AKT/mTOR-mediated autophagy and angiogenesis in Lewis lung carcinoma mouse model. Biomed Pharmacother. 2020;125:109746.
30. Guo RQ, Peng JZ, Li YM, Li XG. Microwave ablation combined with anti-PD-1/CTLA-4 therapy induces an antitumor immune response to renal cell carcinoma in a murine model. Cell Cycle. 2023;22(2):242–54.
31. Shao D, Chen Y, Huang H, et al. LAG3 Blockade coordinates with microwave ablation to promote CD8(+) T cell-mediated anti-tumor immunity. J Transl Med. 2022;20(1):433.
32. Fujimori M, Kimura Y, Ueshima E, et al. Lung ablation with irreversible electroporation promotes immune cell infiltration by sparing extracellular matrix proteins and vasculature: implications for immunotherapy. Bioelectricity. 2021;3(3):204–14.
33. An X, Yu W, Liu J, Tang D, Yang L, Chen X. Oxidative cell death in cancer: mechanisms and therapeutic opportunities. Cell Death Dis. 2024;15(8):556.
34. Fracasso M, Dutra da Silva A, Bottari NB, et al. Resveratrol impacts in oxidative stress in liver during trypanosoma Cruzi infection. Microb Pathog. 2021;153:104800.
35. Fan Y, Mu Y, Lu L, et al. Hydrogen peroxide-inactivated bacteria induces potent humoral and cellular immune responses and releases nucleic acids. Int Immunopharmacol. 2019;69:389–97.
36. Shin M, Chang E, Lee D, et al. Drosophila immune cells transport oxygen through PPO2 protein phase transition. Nature. 2024;631(8020):350–9.

37. Dostert C, Grusdat M, Letellier E, Brenner D. The TNF family of ligands and receptors: communication modules in the immune system and beyond. Physiol Rev. 2019;99(1):115–60.
38. Trapnell C, Cacchiarelli D, Grimsby J, et al. The dynamics and regulators of cell fate decisions are revealed by pseudotemporal ordering of single cells. Nat Biotechnol. 2014;32(4):381–6.
39. Richards DM, Hettinger J, Feuerer M. Monocytes and macrophages in cancer: development and functions. Cancer Microenviron. 2013;6(2):179–91.
40. Chen Y, Song Y, Du W, Gong L, Chang H, Zou Z. Tumor-associated macrophages: an accomplice in solid tumor progression. J Biomed Sci. 2019;26(1):78.
41. Padgett LE, Araujo DJ, Hedrick CC, Olingy CE. Functional crosstalk between T cells and monocytes in cancer and atherosclerosis. J Leukoc Biol. 2020;108(1):297–308.
42. Sanford DE, Belt BA, Panni RZ, et al. Inflammatory monocyte mobilization decreases patient survival in pancreatic cancer: a role for targeting the CCL2/CCR2 axis. Clin cancer Research: Official J Am Association Cancer Res. 2013;19(13):3404–15.
43. Wang Q, Long G, Luo H, et al. S100A8/A9: an emerging player in sepsis and sepsis-induced organ injury. Biomed Pharmacother. 2023;168:115674.
44. Ferretti E, Pistoia V, Corcione A. Role of fractalkine/CX3CL1 and its receptor in the pathogenesis of inflammatory and malignant diseases with emphasis on B cell malignancies. Mediat Inflamm. 2014;2014:480941.
45. Shao F, Gao Y, Wang W, et al. Silencing EGFR-upregulated expression of CD55 and CD59 activates the complement system and sensitizes lung cancer to checkpoint Blockade. Nat Cancer. 2022;3(10):1192–210.
46. Pakvisal N, Kongkavitoon P, Sathitruangsak C, et al. Differential expression of immune-regulatory proteins C5AR1, CLEC4A and NLRP3 on peripheral blood mononuclear cells in early-stage non-small cell lung cancer patients. Sci Rep. 2022;12(1):18439.
47. Mamdani H, Matosevic S, Khalid AB, Durm G, Jalal SI. Immunotherapy in lung cancer: current landscape and future directions. Front Immunol. 2022;13:823618.
48. Guo RQ, Peng JZ, Li YM, Li XG. Microwave ablation combined with anti-PD-1/CTLA-4 therapy induces an antitumor immune response to renal cell carcinoma in a murine model. Cell Cycle. 2023;22(2):242–54.
49. Zhou W, Yu M, Mao X, et al. Landscape of the peripheral immune response induced by local microwave ablation in patients with breast cancer. Adv Sci (Weinh). 2022;9(17):e2200033.
50. Liu X, Zhang W, Xu Y, et al. Targeting PI3Kgamma/AKT pathway remodels LC3-Associated phagocytosis induced immunosuppression after radiofrequency ablation. Adv Sci (Weinh). 2022;9(7):e2102182.
51. Cassioli C, Baldari CT. The expanding arsenal of cytotoxic T cells. Front Immunol. 2022;13:883010.
52. Ribot JC, Lopes N, Silva-Santos B. γδ T cells in tissue physiology and surveillance. Nat Rev Immunol. 2021;21(4):221–32.
53. Silva-Santos B, Mensurado S, Coffelt SB. γδ T cells: pleiotropic immune effectors with therapeutic potential in cancer. Nat Rev Cancer. 2019;19(7):392–404.
54. Que H, Fu Q, Lan T, Tian X, Wei X. Tumor-associated neutrophils and neutrophil-targeted cancer therapies. Biochim Biophys Acta Rev Cancer. 2022;1877(5):188762.
55. Leong TL, Bryant VL. B cells in lung cancer-not just a bystander cell: a literature review. Transl Lung Cancer Res. 2021;10(6):2830–41.
56. Olingy CE, Dinh HQ, Hedrick CC. Monocyte heterogeneity and functions in cancer. J Leukoc Biol. 2019;106(2):309–22.
57. Wang G, Li H, Pan J, et al. Upregulated expression of Cancer-Derived Immunoglobulin G is associated with progression in glioma. Front Oncol. 2021;11:758856.
58. Wen H, Guo D, Zhao Z et al. Novel pyroptosis-associated genes signature for predicting the prognosis of sarcoma and validation. *Biosci Rep.* 2022;42(12).
59. Mon MM, Srisomsap C, Chokchaichamnankit D, et al. Serum proteomic profiling reveals differentially expressed IGHG3 and A1AG1 as potential predictors of chemotherapeutic response in advanced Non-small cell lung cancer. Anticancer Res. 2021;41(4):1871–82.
60. Lohr M, Edlund K, Botling J, et al. The prognostic relevance of tumour-infiltrating plasma cells and Immunoglobulin kappa C indicates an important role of the humoral immune response in non-small cell lung cancer. Cancer Lett. 2013;333(2):222–8.
61. Zhang Y, Shi J, Luo J, Liu C, Zhu L. Metabolic heterogeneity in early-stage lung adenocarcinoma revealed by RNA-seq and scRNA-seq. Clin Transl Oncol. 2023;25(6):1844–55.
62. Capasso M, Durrant LG, Stacey M, Gordon S, Ramage J, Spendlove I. Costimulation via CD55 on human CD4 + T cells mediated by CD97. J Immunol. 2006;177(2):1070–7.
63. Bai J, Ding B, Li H. Targeting TNFR2 in cancer: all roads lead to Rome. Front Immunol. 2022;13:844931.
64. Tang W, Lu Y, Tian QY, et al. The growth factor progranulin binds to TNF receptors and is therapeutic against inflammatory arthritis in mice. Science. 2011;332(6028):478–84.
65. Dunsmore G, Rosero EP, Shahbaz S, et al. Neutrophils promote T-cell activation through the regulated release of CD44-bound Galectin-9 from the cell surface during HIV infection. PLoS Biol. 2021;19(8):e3001387.
66. Wong NK, Lai JC, Birkenhead D, Shaw AS, Johnson P. CD45 down-regulates Lck-mediated CD44 signaling and modulates actin rearrangement in T cells. J Immunol. 2008;181(10):7033–43.
67. He X, Smith SE, Chen S, et al. Tumor-initiating stem cell shapes its microenvironment into an immunosuppressive barrier and pro-tumorigenic niche. Cell Rep. 2021;36(10):109674.
68. Markiewski MM, Vadrevu SK, Sharma SK, et al. The ribosomal protein S19 suppresses antitumor immune responses via the complement C5a receptor 1. J Immunol. 2017;198(7):2989–99.

Publisher's note